



MERIS

Ref.: PO-TN-MEL-GS-0005

Issue: 4.3

Date: 18/07/2011

Page: i

MERIS ATBD 2.13 Sun Glint Flag Algorithm

Ref.: PO-TN-MEL-GS-0005

Issue: 4.3

Date: 18/07/2011



MERIS ATBD 2.13
Sun Glint Flag Algorithm

Ref.: PO-TN-MEL-GS-0005

Issue: 4.3

Date: 18/07/2011

Page: ii

Preparation and signature list

	Name and role	Company	Signature
Prepared by	L. Bourg	ACRI-ST	
	F. Montagner	ACRI-ST	
	V. Billat	ACRI-ST	
	S. Bélanger	ACRI-ST	

Distribution List

Company	To
	Public distribution

Change log

Version	Date	Changes
4.3	18/07/2011	Changes following the 3 rd MERIS data reprocessing: <ul style="list-style-type: none">■ Modification of Eq. 14 (typo)■ Parameters values updated by Ebushi et Kizu in 2002■ References
4.2	10/06/2003	
4.1	18/02/2000	



Table of Content

1	INTRODUCTION	5
2	ALGORITHM OVERVIEW	5
3	ALGORITHM DESCRIPTION	5
3.1	THEORETICAL DESCRIPTION	5
3.1.1	Physics of the problem	5
3.1.2	Mathematical description of the algorithm	8
3.1.3	Parameter description	11
3.1.4	Error budget estimates	11
3.2	PRACTICAL CONSIDERATIONS	12
3.2.1	Calibration and Validation	12
3.2.2	Quality control and diagnostics	12
3.2.3	Exception handling	12
3.2.4	Output Product	12
4	ASSUMPTIONS AND LIMITATIONS	13
4.1	ASSUMPTIONS	13
4.2	LIMITATIONS	13
5	REFERENCES	14



MERIS ATBD 2.13
Sun Glint Flag Algorithm

Ref.: PO-TN-MEL-GS-0005

Issue: 4.3

Date: 18/07/2011

Page: iv

List of Figures

Figure 1: Sun glint geometry	8
Figure 2: Local reference frame	9
Figure 3: Algorithm flow chart	10

List of Tables

Table 1: Parameter description.....	11
-------------------------------------	----

1 Introduction

This document corresponds to the **MERIS ATBD 2.13**: It describes the algorithm used to perform a correction for ocean pixels which are contaminated by Sun glint (specular reflection of Sun light over ocean waves).

Corrected reflectances are inputs to the atmospheric corrections algorithm (ATBD 2.7), and are made available in the MERIS Level 2 Product.

2 Algorithm overview

The glint reflectance estimate algorithm is performed on every ocean pixels in the MERIS data.

It uses external knowledge of the wind speed and direction, and the illumination and observation geometry of each pixel, to estimate the level of Sun glint contribution to the surface reflectance.

- ❖ When that contribution is below a "low threshold" value, it is neglected;
- ❖ When above that threshold and below a "high threshold", it is subtracted from the signal and a "medium glint" flag is raised;
- ❖ When above the "high threshold", pixels are flagged as "high glint" and processed, even if the correction is less reliable. In case the correction yields negative values, it is disabled.

3 Algorithm description

3.1 Theoretical description

3.1.1 Physics of the problem

The estimate of the Sun glint contribution to the ocean signal is based on the Cox and Munk model. These authors have proposed a model that considers the sea surface as a collection of facets, each with individual slope components z_x and z_y . The probability distribution of facet slopes $p(z_x, z_y)$ depends on the wind speed and direction.

In a target-fixed, local coordinates system with the y axis aligned with the Sun azimuth, given the Sun zenith angle θ_s and the sensor zenith angle θ_v and azimuth angle ϕ_v specifying the reflected ray, a wave facet specified by the zenith angle β and azimuth angle α (taken clockwise from the Sun) of its outward normal (Figure 1), the condition for that facet to reflect Sun light in the direction (θ_v, ϕ_v) towards the sensor is:

$$\cos 2\omega = \cos(\theta_v) \cos(\theta_s) + \sin(\theta_v) \sin(\theta_s) \cos(\Delta\phi) \quad (\text{Eq. 1})$$

where ω is the specular reflection angle and $\Delta\phi$ is defined as $\phi_s - \phi_v$.

According to the law of reflection, the vector difference between the reflected and incident rays must lie along the facet normal. From this, it is possible to express the facet angles α and β as a function of the incident and reflected directions.

The angle β formed by the facet normal and the z-axis is computed as:

$$\cos \beta = \frac{\cos \theta_v + \cos \theta_s}{(2 + 2 \cos 2\omega)^{\frac{1}{2}}} \quad (\text{Eq. 2})$$

The azimuth of the facet α measured clockwise from the sun (y-axis) is:

$$\cos \alpha = \frac{-\sin \theta_v \sin \Delta\phi}{\sin \beta (2 + 2 \cos 2\omega)^{\frac{1}{2}}} \quad (\text{Eq. 3})$$

$$\sin \alpha = \frac{(\sin \theta_v \cos \Delta\phi + \sin \theta_s)}{\sin \beta (2 + 2 \cos 2\omega)^{\frac{1}{2}}} \quad (\text{Eq. 4})$$

The slopes of the wave facet in the x and y-directions z_x , z_y can be expressed as a function of the facet azimuth α and zenith β as follows:

$$z_x = \sin \alpha \tan \beta \quad (\text{Eq. 5})$$

$$z_y = \cos \alpha \tan \beta \quad (\text{Eq. 6})$$

which leads to :

$$z_x = \frac{-\sin \theta_v \sin \Delta\phi}{\cos \theta_s + \cos \theta_v} \quad (\text{Eq. 7})$$

$$z_y = \frac{\sin \theta_v \cos \Delta\phi + \sin \theta_s}{\cos \theta_s + \cos \theta_v} \quad (\text{Eq. 8})$$

Let W be the wind speed modulus. It is expressed as:

$$W(j,f) = (W_u(j,f)^2 + W_v(j,f)^2)^{1/2} \quad (\text{Eq. 9})$$

Let χ be the wind direction in the local frame (χ taken clockwise from the sun). If the sun system (x,y) is rotated through an angle χ to a new system (x',y') related to the wind

direction, then the Cox and Munk model provides facet slopes z'_x and z'_y in this wind system as:

$$z'_x = \sin \alpha' \tan \beta \quad (\text{Eq. 10})$$

$$z'_y = \cos \alpha' \tan \beta \quad (\text{Eq. 11})$$

where $\alpha' = \alpha - \chi$

Therefore:

$$z'_x = \cos(\chi) z_x + \sin(\chi) z_y \quad (\text{Eq. 12})$$

$$z'_y = -\sin(\chi) z_x + \cos(\chi) z_y \quad (\text{Eq. 13})$$

and with $\xi = \frac{1}{\sigma_c} z'_x$ and $\eta = \frac{1}{\sigma_u} z'_y$, the probability that the facet reflects specularly the incident radiation in the sensor direction is:

$$p(z'_x, z'_y) = \frac{1}{2\pi\sigma_u\sigma_c} e^{-\frac{\xi^2 + \eta^2}{2}} \left[\begin{array}{l} 1 - (1/2)C_{21}\eta(\xi^2 - 1) - (1/6)C_{03}(\eta^3 - 3\eta) + \\ (1/24)C_{40}(\xi^4 - 6\xi^2 + 3) + (1/4)C_{22}(\xi^2 - 1)(\eta^2 - 1) + \\ (1/24)C_{04}(\eta^4 - 6\eta^2 + 3) \end{array} \right] \quad (\text{Eq. 14})$$

where:

$$\sigma_c(j,f) = (\sigma_c^0 + \sigma_c^1 W)1/2 \text{ with } \sigma_c^0 = 0,003 \text{ and } \sigma_c^1 = 1,92.10^{-3} \quad (\text{Eq. 15})$$

$$\sigma_u(j,f) = (\sigma_u^0 + \sigma_u^1 W)1/2 \text{ with } \sigma_u^0 = 0,000 \text{ and } \sigma_u^1 = 3,16.10^{-3} \quad (\text{Eq. 16})$$

$$C_{21} = C_{21}^0 + C_{21}^1 W \text{ with } C_{21}^0 = 0,01 \text{ and } C_{21}^1 = -0,0086 \quad (\text{Eq. 17})$$

$$C_{22} = 0,12 \quad (\text{Eq. 18})$$

$$C_{03} = C_{03}^0 + C_{03}^1 W \text{ with } C_{03}^0 = 0,04 \text{ and } C_{03}^1 = -0,033 \quad (\text{Eq. 19})$$

$$C_{40} = 0,40 \quad (\text{Eq. 20})$$

$$C_{04} = 0,23 \quad (\text{Eq. 21})$$

The Sun glint reflectance is then:

$$\rho_g(\theta_v, \theta_s, \Delta\phi) = \frac{\pi r(\omega)}{4 \cos \theta_s \cos \theta_v \cos^4 \beta} p(z'_x, z'_y) \quad (\text{Eq. 22})$$

where the Fresnel reflection coefficient $r(\omega)$ can be considered as a constant (0,02) for incidence between 0 and 50 degrees.

Values of parameters listed above are those of the original Cox & Munk publication (1954). Ebuchi and Kizu (2002) have proposed a reviewed parameterisation of the probability distribution function from Geostationary Meteorological Satellite (GMS) and vectors winds observed by scatterometers. We recommend using their linear regressions for σ_c and σ_u :

- ❖ $\sigma_c^0 = 0,0048$ and $\sigma_c^1 = 1.52 \cdot 10^{-3}$
- ❖ $\sigma_u^0 = 0,0053$ and $\sigma_u^1 = 6.71 \cdot 10^{-4}$

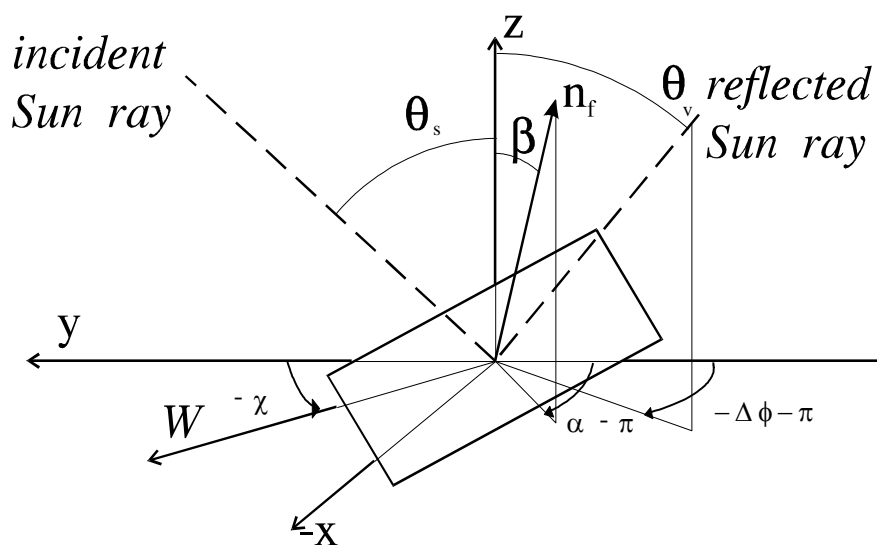


Figure 1: Sun glint geometry

3.1.2 Mathematical description of the algorithm

The Sun glint reflectance observed by MERIS is estimated at each ocean pixel taking as inputs:

- ❖ The Sun zenith and azimuth angles, observer zenith and azimuth angles at the pixel, interpolated from the level 1 product annotation at the nearest tie points;
- ❖ The wind at 10m vector in the local frame, taken at the nearest tie point.

The local reference frame F_L is defined at the pixel, with the x axis pointing Eastward, the y-axis pointing Northward and the z-axis aligned with the outward local normal (Figure 2).

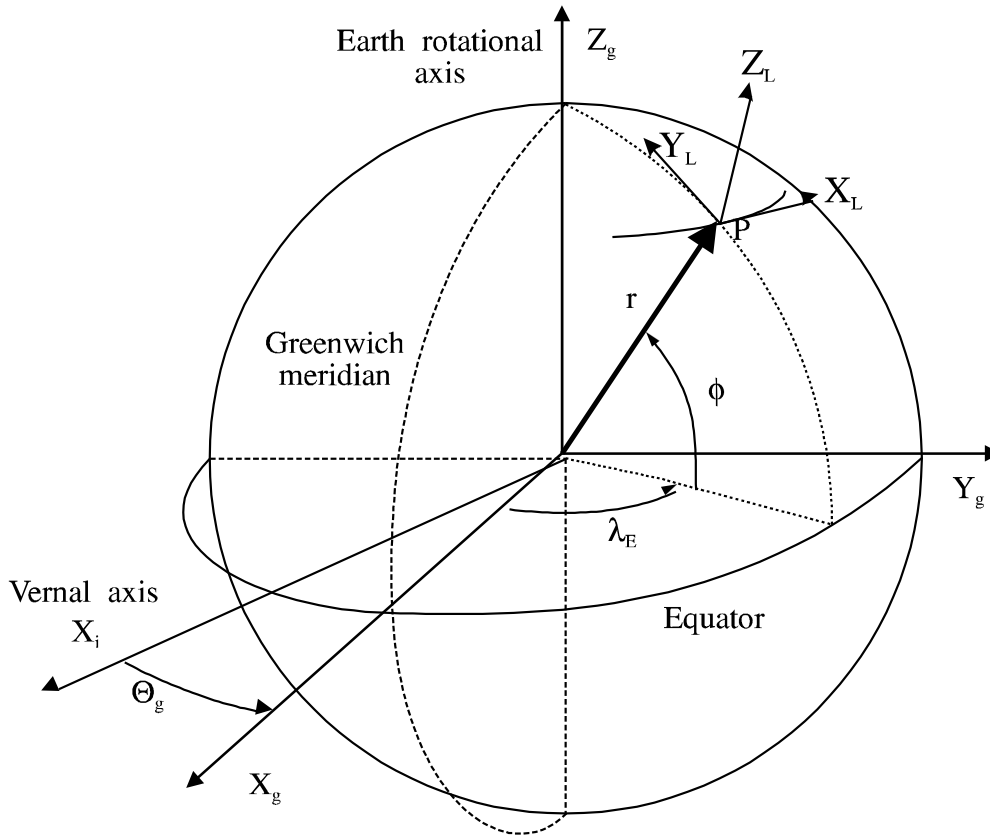


Figure 2: Local reference frame

The Sun glint reflectance is estimated following the development in § 3.1.1 above. It is then converted to TOA reflectance ρ_g^* using an estimate of atmospheric transmittance:

$$t = \exp(-(\tau_R(b,j,f) + \tau_{oz}(b,j,f))/\cos(\theta_s(j,f))) \exp(-(\tau_R(b,j,f) + \tau_{oz}(b,j,f))/\cos(\theta_v(j,f)))$$

$$\rho_g^* = t \rho_g$$

If ρ_g^* in [GLINT_THR_LOW... GLINT_THR_HIGH]

Then $\rho_T' = \rho_T - \rho_g^* + \text{GLINT_THR_LOW}$ and MeGlint = TRUE

if $\rho_g^* > \text{GLINT_THR_HIGH}$

then HighGlint = FALSE.

Values for GLINT_THR_LOW and GLINT_THR_HIGH are determined following tests of the Atmospheric Correction above water (see ATBD 2.7) in presence of increasing amount of glint. GLINT_THR_LOW is fixed at the lowest level where glint influences the results of the atmospheric correction. GLINT_THR_HIGH depends on the value of the TOA reflectance at 865 nm (the band most sensitive to glint in the atmospheric correction): glint correction is

disabled when ρ^*_g exceeds a specified fraction (0.8) of the observed reflectance. In such case, all level 2 products except water vapour should be flagged.

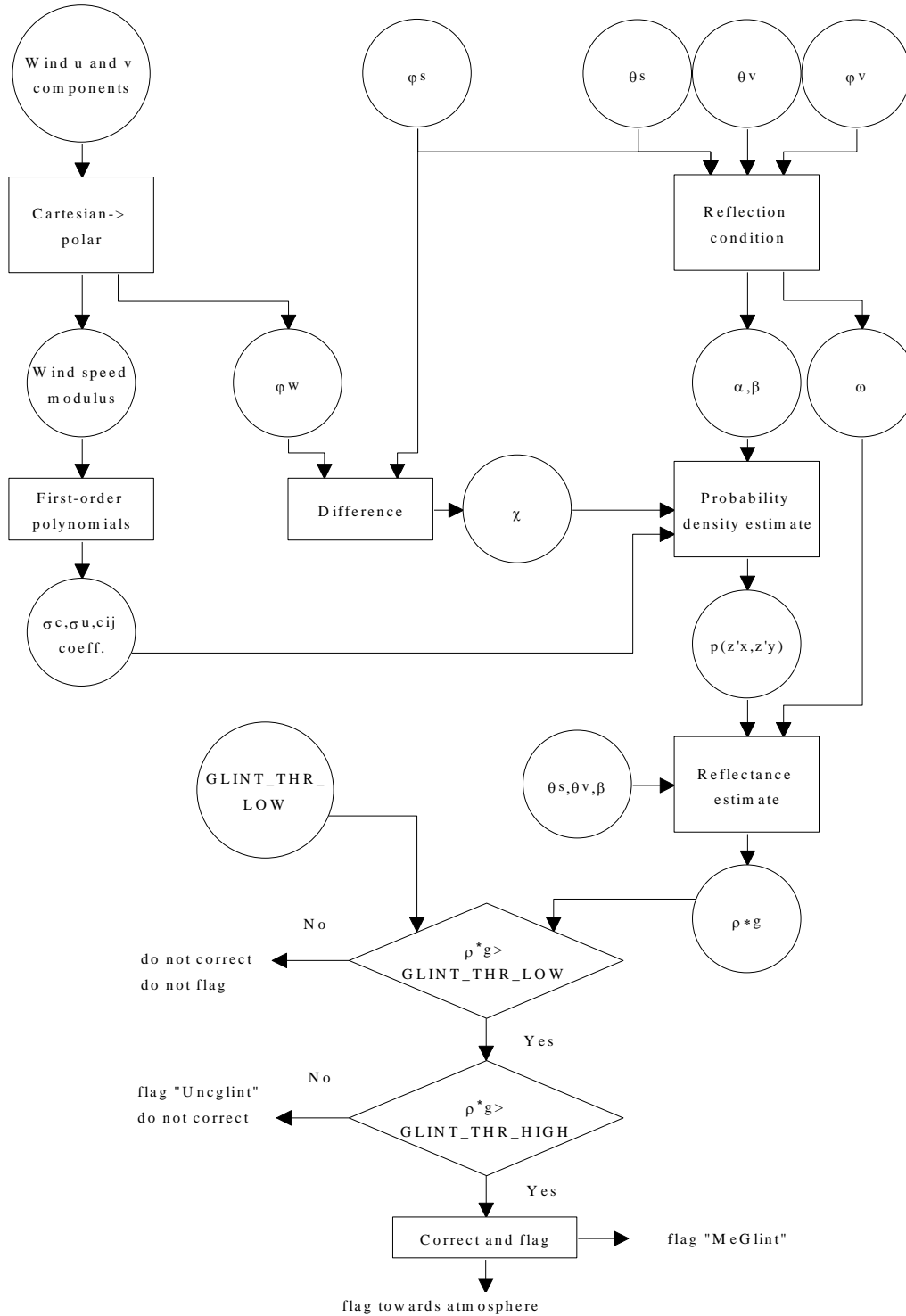


Figure 3: Algorithm flow chart

3.1.3 Parameter description

Table 1: Parameter description (i=input ; c=intermediate computed parameter ;o=ouput)

Symbol	Descriptive name	I/O	Origin
$\theta_s[j,f]$	Sun zenith angle for pixel j,f	i	interpolated from Level 1b product tie points
$\phi_s[j,f]$	Sun azimuth for pixel j,f	i	interpolated from Level 1b product tie points
$\theta_v[j,f]$	Observer zenith angle for pixel j,f	i	interpolated from Level 1b product tie points
$\phi_v[j,f]$	Sensor azimuth for pixel j,f	i	interpolated from Level 1b product tie points
W_u, W_v	Wind vector components	i	interpolated from Level 1b product tie points
σ_c^0, σ_c^1	Polynomial coefficients for σ_c	i	$\sigma_c^0 = 0.0048$ $\sigma_c^1 = 0.00152$
σ_u^0, σ_u^1	Polynomial coefficients for σ_u	i	$\sigma_u^0 = 0.0053$ $\sigma_u^1 = 0.000671$
C_{21}^0, C_{21}^1	Polynomial coefficients for C_{21}	i	$C_{21}^0 = 0.01$ $C_{21}^1 = -0.0086$
C_{03}^0, C_{03}^1	Polynomial coefficients for C_{03}	i	$C_{03}^0 = 0.04$ $C_{03}^1 = -0.033$
C_{40}, C_{22}, C_{04}	Weighting factors in $p(z'_x, z'_y)$	i	$C_{40}=0.4$ $C_{22}=0.12$ $C_{04}=0.23$
$r(\omega)$	Fresnel reflection factor	i	0.022
GLINT_THR_LOW	Threshold for low glint	i	$5.0 \cdot 10^{-4}$
GLINT_THR_HIGH	Threshold for high glint	i	0.2
ρ_g	Reflectance estimate at surface	c	
ρ_g^*	Reflectance estimate at TOA	c	
T	Atmospheric transmittance	c	
MEGLINT_F(j,f)	Flag for medium glint	o	
HIGHGLINT_F(j,f)	Flag for uncorrected glint	o	

3.1.4 Error budget estimates

Because of

- ❖ The uncertainty on wind from ECMWF global models (typically $2 \text{ m}\cdot\text{s}^{-1}$ on wind speed);

- ❖ The error bars of the Cox and Munk model,

there is an uncertainty in the determination of ρ_g . The value of GLINT_THR_LOW should be established taking that uncertainty into account so as to avoid "over correcting".

The value of GLINT_THR_HIGH will be established taking the saturation of the aerosol correction dedicated channels (705, 775, 865 nm) into account: It is not worth correcting these pixels for glint.

3.2 Practical considerations

3.2.1 Calibration and Validation

The value of GLINT_THR should be established using:

1. Simulation results, establishing the Sun glint sensitivity threshold of the atmosphere correction algorithm;
2. Airborne images of reflectance (a high spectral resolution is not necessary).

The glint reflectance estimate may be implemented in Look-Up Tables.

3.2.2 Quality control and diagnostics

The PCD in the Level 1 product header, indicating the quality of the available wind data, should be repeated in the Level 2 product header to notify the likely error in the size of the Sun glint patch.

3.2.3 Exception handling

N/A

3.2.4 Output Product

The output of the algorithm is a boolean flag for each pixel of the frame: Glint_ff[j,f]. When true, that flag indicate that the pixel is (most likely) meaningfully affected by Sun glint and should not be processed further. Another flag indicates when the correction has been applied.

4 Assumptions and Limitations

4.1 Assumptions

No further assumptions than mentioned in 3.1 above.

4.2 Limitations

This algorithm accepts as an established reference the Cox and Munk model. That model does not provide a complete description of the wave slope distribution:

1. Swell, not related to local wind, is not taken into account;
2. The model is valid for a deep ocean where interaction with the sea bottom is negligible. In reality, the wave profile is distorted when the sea bottom gets close to the surface.

5 References

- [1] Cox, C.; Munk, W. Statistics of the Sea Surface Derived from Sun Glitter. J. Mar. Res. 1954, 13, 198-227.
- [2] Cox, C.; Munk, W. Measurement of the Roughness of the Sea Surface from Photographs of the Sun's Glitter. J. Opt. Soc. Am. 1954, 44, 838-850.
- [3] Ebuchi, N.; Kizu, S. Probability Distribution of Surface Wave Slope Derived Using Sun Glitter Images from Geostationary Meteorological Satellite and Surface Vector Winds from Scatterometers. J. Oceanogr. 2002, 58, 477-486.



MERIS ATBD 2.13
Sun Glint Flag Algorithm

Ref.: PO-TN-MEL-GS-0005

Issue: 4.3

Date: 18/07/2011

Page: 15

ATBD 2.13 — MERIS DATA PRODUCT SUMMARY SHEET

Product Name: Sun Glint Flag Algorithm
Product Code: SUNGLINT
Product Level: 2
Description of the product: The product is a flag indicating the occurrence of sun glint contamination

Product Parameters:

Coverage: global
Packaging:
Units: no
Range:
Sampling: pixel by pixel
Resolution: radiometric: N/A
spatial: full
Accuracy:
Geo-location Requirements: yes
Format: 2 bits / sample
Appended Data:
Frequency of generation: 1 product per orbit
Size of the Product:

Additional Information:

Identification of bands used in algorithm: 865nm
Assumptions on MERIS input data: None
Identification of ancillary and auxiliary data: Wind vector, illumination and viewing zenith and azimuth angles
Assumptions on ancillary and auxiliary data: Available at input Level 1B product tie points
Input from other ENVISAT instruments: None

End of Document